The Astrophysical Journal, 704:L113–L117, 2009 October 20 doi:10.1088/0004-637X/704/2/L113

CORONAE AS A CONSEQUENCE OF LARGE-SCALE MAGNETIC FIELDS IN TURBULENT ACCRETION DISKS

Eric G. Blackman[1] and Martin E. Pessah[2]
[1] Department of Physics and Astronomy, University of Rochester, Rochester, NY 14627, USA; blackman@pas.rochester.edu
[2] Institute for Advanced Study, Princeton, NJ 08540, USA; mpessah@ias.edu
Received 2009 July 12; accepted 2009 September 16; published 2009 October 5

ABSTRACT

Non-thermal X-ray emission in compact accretion engines can be interpreted to result from magnetic dissipation in an optically thin magnetized corona above an optically thick accretion disk. If coronal magnetic field originates in the disk and the disk is turbulent, then only magnetic structures large enough for their turbulent shredding time to exceed their buoyant rise time survive the journey to the corona. We use this concept and a physical model to constrain the minimum fraction of magnetic energy above the critical scale for buoyancy as a function of the observed coronal to bolometric emission. Our results suggest that a significant fraction of the magnetic energy in accretion disks resides in large-scale fields, which in turn provides circumstantial evidence for significant non-local transport phenomena and the need for large-scale magnetic field generation. For the example of Seyfert active galactic nuclei, for which ∼30% of the bolometric flux is in the X-ray band, we find that more than 20% of the magnetic energy must be of large enough scale to rise and dissipate in the corona.

Key words: accretion, accretion disks – black hole physics – instabilities – MHD – turbulence

1. INTRODUCTION

Gaseous accretion disks around stars or compact objects provide a likely source of emission from these engines (see, e.g., Frank et al. 2002). To explain the rapid variability and short lifetimes of accreting systems without unphysical mass densities, some enhanced angular momentum transport beyond that which can be supplied by microphysical transport coefficients is typically required (Shakura & Sunyaev 1973). Many accreting sources show jets, outflows, and active coronae highlighting that disk dynamics and energy release involves some combination of local and large-scale transport. Understanding the relative balance between the two is of fundamental importance.

In some models, the primary angular momentum transport and dissipation takes place above the disk (Lynden-Bell 1969; Field & Rogers 1993) and the turbulence within the disk plays a secondary role. However, the magnetorotational instability (MRI) has emerged as a likely source of turbulence within accretion disks, and a leading candidate to contribute local turbulent angular momentum transport when they are sufficiently ionized (Velikhov 1959; Chandrasekhar 1960; Balbus & Hawley 1991, 1998). Three-dimensional numerical simulations (Hawley et al. 1995, 1996; Brandenburg et al. 1995; Stone et al. 1996) have revealed that the nonlinear evolution of systems unstable to the MRI can sustain MHD turbulence and outward angular momentum transport.

Understanding the MRI saturation is a topic of active research (see Pessah & Goodman 2009, and references therein). Local shearing box simulations have not converged to practical angular momentum transport coefficients as they are found to depend on the simulation box size, the initial seed magnetic field (see, e.g., Hawley et al. 1995; Sano et al. 2004; Pessah et al. 2007), and the magnetic Prandtl number (Fleming et al. 2000; Sano & Inutsuka 2001; Fromang & Papaloizou 2007; Fromang et al. 2007; Lesur & Longaretti 2007). A frontier is to understand the stronger prevalence of large-scale magnetic field structures in saturation states of stratified MRI-driven turbulence (Brandenburg et al. 1995; Miller & Stone 2000; Suzuki & Inutsuka 2009; Davis et al. 2009; Shi et al. 2009) compared to unstratified cases (e.g., Fromang & Papaloizou 2007) and the role of larger boxes and aspect ratios (Bodo et al. 2008; Davis et al. 2009). A real accretion engine involves coupled internal and coronal dynamics (e.g., Kuncic & Bicknell 2004; Blackman 2007).

Observationally, the relevance of large-scale magnetic fields in accretion disks is motivated by the interpretation of X-rays from Seyferts which has been best interpreted as coronal emission. The flux from 1 to 500 keV ranges from 10% to 50% of the total flux (Mushotzky et al. 1993). Galactic black hole X-ray sources show both thermal and non-thermal (power law) spectral components, with the ratio of non-thermal to total luminosity ranging between 20% and 40% (Nowak 1995). The leading paradigm for X-ray emission in these accreting systems involves an optically thin, hot corona powered by magnetic field dissipation (e.g., Haardt & Maraschi 1993; Field & Rogers 1993; Pariev et al. 2008). If the corona results from magnetic structures dissipating above the disk midplane that were originally produced within the turbulent disk (e.g., via some MRI), then these structures must be of large enough scale to survive the buoyant rise without being prematurely shredded by disk turbulence.

If all coronal and jet emission results from fields initially produced within a turbulent disk, then the fraction of coronal to bolometric luminosity is directly related to the fraction of magnetic energy associated with buoyant fields of large enough scale to survive the vertical trip without being turbulently shredded. In this Letter, we employ this concept and develop a model relating the observed ratio of coronal to bolometric emission to the fraction of magnetic energy produced in the disk that is of large enough scale to buoyantly rise to the corona. By comparing the model implications with observations, we infer that a substantial fraction of magnetic energy in accretion disks is produced in large-scale fields.

2. WHY CORONAE REQUIRE LARGE-SCALE FIELDS

In order for magnetic fields to power coronae and jets, the buoyancy time, t_b, associated with a magnetic structure rising through the disk must be smaller than the time associated with

its turbulent diffusion, t_d. These timescales are estimated as $t_b \equiv H/U_b$, where H is the disk half thickness and U_b is the characteristic buoyancy speed, and $t_d \equiv l^2/\nu_t$, where $\nu_t \sim v l_t$ is the turbulent magnetic diffusion coefficient, v is the dominant turbulent speed, and l_t is the characteristic scale of a typical (anisotropic) turbulent cell, i.e., $l_t \sim \langle l_x l_y l_z \rangle^{1/3}$.

The escape condition, $t_b < t_d$, sets a lower bound on the scale l of magnetic structures that can survive shredding and reach the corona (Blackman & Tan 2004), namely,

$$l^2 > l_c^2 \equiv l_t H \frac{v}{U_b}. \tag{1}$$

Shear can make an initially isotropic structure anisotropic, as can the formation of flux tubes. Thus, the critical scale applies to the *smallest* dimension of a given magnetic structure, i.e., $l_c \leqslant \min\{l_x, l_y, l_z\}$, since this determines the shortest diffusion time.[3]

In the α-viscosity disk framework (Shakura & Sunyaev 1973), $\nu_t \equiv v l_t \equiv \alpha c_s H \sim v^2/\Omega$, where c_s is the sound speed and Ω is the local angular frequency. Using $c_s \sim \Omega H$, this implies $v = \alpha^{1/2} c_s$ and thus $l_t \sim \alpha^{1/2} H$. Plugging these into Equation (1) implies

$$l_c^2 \equiv \alpha H^2 \frac{c_s}{U_b(l_c)}. \tag{2}$$

In a fully developed MHD/MRI turbulent flow the velocity of dominant turbulent motions is approximately (if not slightly less than) the rms Alfvén speed, i.e., $v \sim v_A$. Therefore, if $U_b \leqslant v_A \sim v \sim \alpha^{1/2} c_s$, then $l > l_c > \alpha^{1/4} H = l_t/\alpha^{1/4}$, which is larger than l_t for $\alpha < 1$. If instead we use $U_b(l) \leqslant c_s$, the analogous procedure gives $l > l_c > \alpha^{1/2} H = l_t$. Either way, the buoyant magnetic structures that survive turbulent shredding must have $l > l_c \geqslant l_t$.

That $l_c \geqslant l_t$ implies that an accretion engine with significant power emanating from its corona requires a significant fraction of magnetic energy to be organized in magnetic structures with $l > l_c$. In what follows, we quantify this fraction by determining l_c and $U_b(l)$ and connect them with the observed ratio of coronal to bolometric emission flux.

3. CORONAL EMISSION FRACTION

We develop a model in which the observed fraction of coronal to bolometric disk luminosity is determined by the rate of large-scale magnetic energy rising to the corona. We assume that buoyant structures fill a volume fraction f_v in the disk such that the average disk mass density is

$$\rho \equiv \rho_o - f_v(\rho_o - \rho_i), \tag{3}$$

where ρ_o and ρ_i are the mass densities external to and internal to buoyant structures, respectively. The average magnetic energy density is then

$$\frac{B^2}{8\pi} \equiv \frac{1}{8\pi}\left(B_o^2 + f_v B_{ls}^2\right), \tag{4}$$

where $B_{ls}^2 \equiv B_i^2 - B_o^2$ corresponds to the difference of internal and external magnetic fields squared. We suppose that although the entire magnetic energy of the structures B_i^2 contributes to their initial buoyancy, only B_{ls}^2 survives to the corona; the smaller scale fields are "bled" away during the buoyant rise. We define the fraction of the magnetic energy density in scales larger than the critical scale for surviving the buoyant rise to be

$$f_s \equiv \frac{f_v B_{ls}^2}{B^2} = \frac{f_v B_{ls}^2}{f_v B_{ls}^2 + B_o^2}. \tag{5}$$

The factor f_v arises in the numerator because B_{ls}^2 is contained only in the volume of the buoyant structures. The quantity f_s represents the fraction of magnetic energy with scales larger than l_c, which can be written more generally in terms of integrated magnetic spectra as

$$f_s = \frac{\int_{k_{min}}^{k_c} E_M(k)dk}{\int_{k_{min}}^{k_{max}} E_M(k)dk}, \tag{6}$$

where the limiting wavenumbers are $k_c = 2\pi/l_c$, $k_{min} = 2\pi/H$, and $k_{max} = 2\pi/l_{diss}$ and l_{diss} is the dissipation scale.

Motivated by the physical picture described above, we break up the accretion energy per unit area dissipated at a given radius into the sum of the dissipation associated with small-scale field within the disk

$$D_d \equiv Q\Sigma\Omega^2 \nu_t (1 - f_s) = 2Q\alpha\beta c_s \epsilon_{mag}(1 - f_s), \tag{7}$$

and the dissipation of large-scale field in the corona

$$D_c \equiv f_s U_b \epsilon_{mag}. \tag{8}$$

Here, Σ is the surface density, $Q \equiv (d\ln\Omega/dR)^2/2$ and $\beta \equiv \rho c_s^2/2\epsilon_{mag}$, where $\epsilon_{mag} \equiv B^2/8\pi$ is the total magnetic energy density. The first term on the right-hand side of Equation (7) resembles that which would follow from standard disk theory (Frank et al. 2002) but with the extra factor of $1 - f_s$.

Defining the ratio of coronal to total dissipation as

$$q \equiv \frac{D_c}{D_d + D_c}, \tag{9}$$

the ratio of coronal to disk dissipation becomes

$$\frac{D_c}{D_d} = \frac{q}{1-q} = \frac{f_s}{2Q\alpha\beta(1 - f_s)} \frac{U_b}{c_s}, \tag{10}$$

and depends cleanly on U_b/c_s. Since both D_c and D_d are expected to be dominated by their contributions near the inner radius, we do not address the radial dependence of these quantities in detail here and interpret q as an estimate of total coronal to bolometric emission.

4. CONSTRAINING THE BUOYANCY SPEED

To constrain U_b/c_s, we consider forces on a magnetic structure in pressure balance with its exterior, i.e.,

$$\frac{B_i^2}{8\pi} + n_i k_B T_i = \frac{B_o^2}{8\pi} + n_o k_B T_o, \tag{11}$$

[3] During the rise of a structure, its buoyancy and diffusion times can evolve over multiple scale heights via competing actions involving shear, expansion, and density and magnetic field gradients. The timescales are more precisely represented as integrals over height in a dynamical theory. Here we simply make the comparison at the midplane and for a single scale height. In Section 6, we point out that this gives a lower limit on the large-scale field fraction.

where n and T are the corresponding number densities and temperatures, and k_B is the Boltzmann constant. Assuming $T_i = T_o = T$, we obtain

$$\rho_o - \rho_i = \frac{B_{ls}^2}{8\pi c_s^2}\,. \tag{12}$$

We take the force density acting on the magnetic structure to be $F_b - F_{dr}$, where F_b is the upward gravitational buoyancy force density and F_{dr} is the drag force density. The former can be estimated as

$$F_b \equiv gH\frac{B_{ls}^2}{8\pi c_s^2} = \frac{B_{ls}^2}{8\pi H}\,, \tag{13}$$

where the last equality follows from hydrostatic equilibrium for an isothermal gas ($\Gamma = 1$), that is $k_B T/m_p = c_s^2 = (GM/R)(H/R)$, with $g \equiv GM/R^2$. We approximate F_d to be the high Reynolds number hydrodynamic drag associated with a cylinder of length L and diameter l, namely (see, e.g., Moreno-Insertis 1986; Landau & Lifshitz 1987)

$$F_{dr} \equiv \frac{C_{dr}}{2}\rho_o U_b^2\left[\frac{lL}{\pi(l/2)^2 L}\right] = \frac{2C_{dr}}{\pi l}\rho_o U_b^2\,, \tag{14}$$

with drag coefficient C_{dr} of order unity. The work done per unit volume by the net force over a distance H equals the kinetic energy density of the rising structure, $H(F_{dr} - F_b) \simeq \rho_i U_b^2/2$. Combining this with Equations (12)–(14), we obtain

$$\frac{U_b}{c_s} = \left(1 - \frac{\rho_i}{\rho_o}\right)^{1/2}\left(\frac{2C_{dr}}{\pi}\frac{H}{l} + \frac{\rho_i}{2\rho_o}\right)^{-1/2}\,. \tag{15}$$

Therefore, for all buoyant structures $U_b(l) \geqslant U(l_c)$ since $l \geqslant l_c$. Given that $l \leqslant H$ for all structures that fit in the disk, $U_b(l) < c_s$ for all l would imply $\rho_i/\rho_o > 2/3 - 4C_{dr}/3\pi$. We thus restrict ourselves to this density ratio regime. Note that our estimate for U_b/c_s is itself an upper limit since we consider only a hydrodynamic drag force restricting the buoyant rise, ignoring for example, magnetic tension, compared to Schramkowski & Torkelsson (1996). Whether the dynamics allows densities below the above upper limit remains an open question. However, even if the structures were initially moving faster than c_s, shocks and the associated dissipation would slow the motion via additional drag.

Vishniac (1995) estimated $U_b \sim \alpha c_s$. Had we used this smaller $U_{,b}$ instead of the upper limit c_s, our value of f_s in Equation (17) would dramatically increase, highlighting the importance of large-scale field for coronal dynamics even more. Characteristic values of f_s resulting from this smaller buoyancy speed are shown as dashed lines in Figure 2.

5. QUANTIFYING THE IMPORTANCE OF LARGE-SCALE FIELDS

Setting $l = l_c$ in Equation (15), and using Equation (2), gives a fifth-order equation for l_c/H as a function of C_{dr}, ρ_i/ρ_o, and α. The physical solution to this equation is shown in Figure 1 for a range in drag coefficients, $10^{-3} \leqslant C_{dr} \leqslant 2$, and for three values of $\alpha = \{0.5, 0.1, 0.01\}$ as a function of the density ratio ρ_i/ρ_o. The characteristic turbulent scale $l_t \equiv \alpha^{1/2}H$ is also shown as horizontal lines for each value of α. Since l_c is the minimum scale for buoyant rise, the fact that $l_c > l_t$ highlights the importance of large-scale fields. For the regime

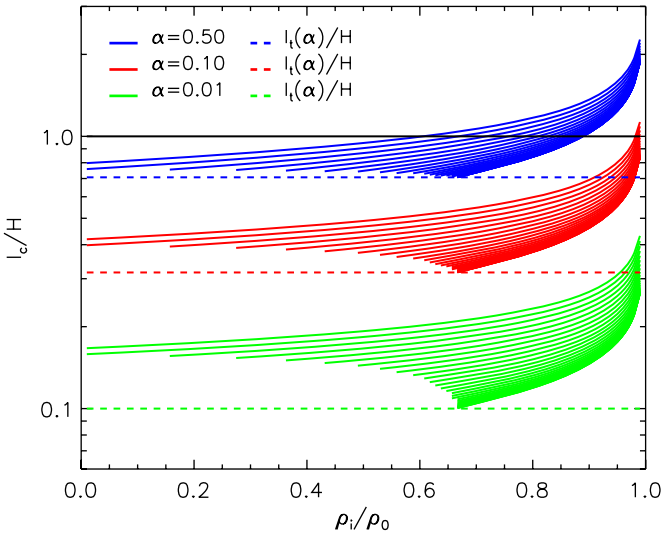

Figure 1. Ratio of the critical scale for buoyancy to the disk scale height, l_c/H, that satisfies Equations (2) and (15) simultaneously, as a function of the density ratio ρ_i/ρ_o. The three sets of solid curves correspond to $\alpha = \{0.5, 0.1, 0.01\}$ from top to bottom. Larger values of α correspond to more efficient shredding and thus require larger scales l_c to survive the buoyant rise. For a given α, the solutions correspond to a range of drag coefficients $10^{-3} \leqslant C_{dr} \leqslant 2$, logarithmically spaced. The bottommost curves in each set correspond to the lowest drag; larger C_{dr} requires a larger l_c to survive buoyant rise. The dashed lines show the turbulent scale $l_t = \alpha^{1/2}H$. That each set of curves lies above the line associated with $l_t(\alpha)$ shows the importance of large-scale fields. A corona cannot form for region $l_c > H$.

on the plot where $l_c > H$, a buoyant corona cannot arise from fields produced internally to the disk.

We can set two constraints on the minimum fraction f_s of magnetic energy that the disk must produce in fields with scales $l > l_c$ for a given coronal to bolometric emission fraction q. The more stringent bound relies on the fact that $U_b(l) < U_b(H)$ for $l < H$; a less severe limit is obtained requiring $U_b(H) < c_s$, which is satisfied as long as the density ratio ρ_i/ρ_o does not fall below the lower limit discussed above. Applying these conditions to Equation (10), we obtain

$$\frac{D_c}{D_d} = \frac{q}{1-q} \leqslant \frac{f_s U_b(H)/c_s}{2Q\alpha\beta(1-f_s)} \leqslant \frac{f_s}{2Q\alpha\beta(1-f_s)}\,. \tag{16}$$

Then, for an observationally inferred value of coronal to bolometric flux, we can obtain a lower limit on the fraction of magnetic energy residing in large-scale fields, i.e.,

$$f_s \geqslant \frac{\alpha\beta}{\alpha\beta + 4(1/q - 1)/9}\,, \tag{17}$$

where we have used $Q \sim 9/8$ for Keplerian disks.

The lower limit for f_s depends on the dimensionless parameters characterizing the angular momentum transport efficiency, α, and magnetic pressure support, β, *only* though the product $\alpha\beta$. This is encouraging because, despite the fact that both quantities vary over several orders of magnitude across simulations carried out in domains with various sizes and with different field strengths and geometries (see Pessah et al. 2006, and references therein), their product remains nearly constant[4] with $\alpha\beta \simeq 0.5$ (see Blackman et al. 2008, and references therein).

[4] The constancy of $\alpha\beta$ is consistent with the relations below Equation (2); for a disk with MRI growth time $\sim\Omega^{-1}$, we expect $\nu_t = \alpha c_s H \sim v^2/\Omega \sim v_A^2/\Omega$. Using $c_s \sim \Omega H$ then gives $\alpha \propto \beta^{-1}$ with a proportionality constant dependent upon anisotropy and the polytropic index (Blackman et al. 2008).

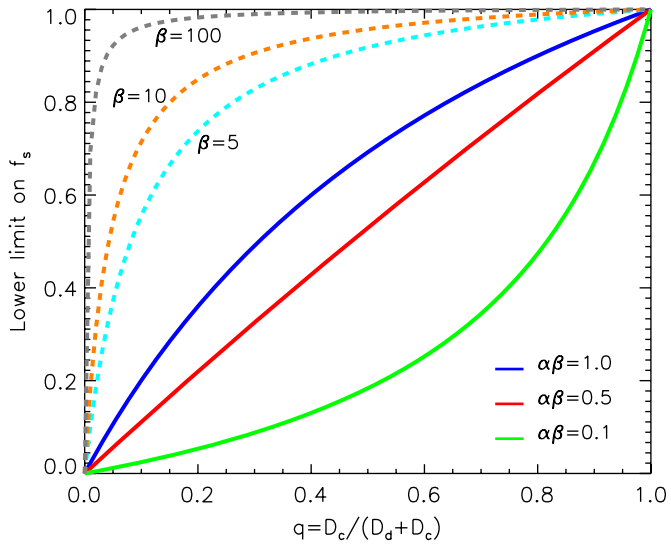

Figure 2. Lower limits on the fraction of magnetic energy residing at scales large enough for their buoyant rise time to be small compared to the corresponding turbulent shredding time, f_s, as a function of the ratio of coronal to bolometric dissipation, q. The solid curves correspond to $U_b = c_s$ in Equation (16) which gives the most stringent lower limit for $\alpha\beta = \{1.0, 0.5, 0.1\}$, from top to bottom. The dashed curves correspond to $U_b = \alpha c_s$, as suggested in Vishniac (1995). In this case, the lower limit given by Equation (16) is independent of α. The dashed lines correspond to $\beta = \{100, 10, 5\}$, from top to bottom ($\beta = 1$ would coincide with the curve for $\alpha\beta = 1$ for $U_b = c_s$). This last set of curves show that the same ratio of coronal to bolometric emission requires a higher fraction of large-scale fields as the buoyancy speed is reduced.

The upper limits for the fraction of magnetic energy associated with large-scale field structures are shown in Figure 2 for three values of the product $\alpha\beta = \{1.0, 0.5, 0.1\}$. The minimum constraints on f_s show that if the observed non-thermal emission is interpreted as coronal emission due to magnetic dissipation from buoyant fields that were produced within a turbulent disk, then a significant fraction of the energy budget of the magnetic field build in the disk must be produced in fields of scale $l > l_c$. Since Figure 1 shows that in general $l > l_t$, together these figures highlight the importance of large-scale magnetic fields in powering coronae.

Finally, we note that MHD jet models typically invoke global scale fields, compared to Ferreira (2007). If these fields arise from the opening of coronal fields (as in the Sun; Wang & Sheeley 2003: Blackman & Tan 2004) then the mechanical luminosities of jets would represent an additional contribution to that which results from the buoyant rise of magnetic fields. Specifically, D_c in Equation (9) would be replaced by $D_c + D_j$ where the latter is the jet power. This would further increase our lower limits on f_s.

6. RELATION TO PREVIOUS WORK

In our physical picture, the coronal emission fraction q depends on the fraction of magnetic energy f_s produced in scales larger than the critical scale l_c. We incorporate the density contrast between buoyant structures and the ambient medium required for coronal feeding. Also, our lower limit on f_s employs c_s as an upper limit for the buoyant rise time. We use the α-viscosity prescription only for dissipation inside the disk; the coronal dissipation is modeled as a distinct contribution (see Equations (7) and (8)). These features differ from those of Merloni & Fabian (2002) and Wang et al. (2004) which make no distinction between the density inside and outside the buoyant structures or the role of large-scale versus small-scale magnetic fields. Furthermore, the coronal emission fraction in those papers is taken as a subset of the viscous (α-viscosity) dissipation. Also, the buoyant rise time is taken to be the Alfvén speed; less than our upper limit value of c_s.

In the present work, we implicitly consider systems with low enough accretion rates such that radiation pressure is unimportant. A subtlety associated with radiation pressure is that the thermal photosphere can be significantly higher than the scale at which the magnetic pressure dominates the thermal pressure (e.g., Hirose et al. 2009) reducing the observationally inferred coronal non-thermal emission fraction. This reduction for large accretion rate systems is observed in Wang et al. (2004). For a fixed magnetic spectrum, this would also be expected in our paradigm, because H in Equation (2) is the scale that we consider a buoyant structure must rise to contribute to coronal emission. If the buoyant structure has to move higher, then l_c would be larger and less of the magnetic energy would survive the buoyant rise. In Merloni & Fabian (2002), the reduction in coronal emission for large radiation pressure occurs because their coronal emission fraction depends inversely on the total disk pressure.

7. CONCLUSIONS

Starting with the assumption that coronal luminosity from a turbulent accretion disk results from buoyant magnetic structures that survive turbulent shredding for at least one vertical density scale height, we derived lower limits on (1) the scale of such magnetic structures and (2) the fraction of magnetic energy that needs to be produced above this scale within the disk to account for observed values of coronal to bolometric luminosity. In our minimalist model, we considered the buoyant structures to be in pressure equilibrium with the ambient medium but to have an additional magnetic energy contribution from scales above the critical scale l_c, and a lower density.

We find that typical ratios of coronal to bolometric luminosity observed in active galactic nuclei require the critical scale for buoyancy to robustly exceed the characteristic scale set by turbulent motions and that double-digit percentages of magnetic energy should reside in fields above this scale. This is consistent with recent work highlighting the importance of in situ large-scale dynamos in feeding coronae (Blackman 2007; Vishniac 2009). Our results complement growing motivation to consider larger domains in stratified MRI simulations and motivate analysis of the magnetic energy spectra produced therein. The results also resonate with models of accretion disks in which buoyancy and coronal dissipation play a primary role for transport (Lynden-Bell 1969; Field & Rogers 1993).

We thank J. Goodman, A. Hubbard, V. Pariev, and D. Uzdensky for related discussions. E.G.B. acknowledges NSF grants AST-0406799, AST-0406823, and NASA grant ATP04-0000-0016 and the LLE at UR. M.E.P. gratefully acknowledges support from the Institute for Advanced Study.

REFERENCES

Balbus, S. A., & Hawley, J. F. 1991, ApJ, 376, 214
Balbus, S. A., & Hawley, J. F. 1998, Rev. Mod. Phys., 70, 1
Blackman, E. G. 2007, New J. Phys., 9, 309
Blackman, E. G., Penna, R. F., & Varnière, P. 2008, New Astron., 13, 244
Blackman, E. G., & Tan, J. C. 2004, Ap&SS, 292, 395
Bodo, G., Mignone, A., Cattaneo, F., Rossi, P., & Ferrari, A. 2008, A&A, 487, 1

Brandenburg, A., Nordlund, A., Stein, R. F., & Torkelsson, U. 1995, ApJ, 446, 741
Chandrasekhar, S. 1960, Proc. Natl Acad. Sci., 46, 253
Davis, S. W., Stone, J. M., & Pessah, M. E. 2009, ApJ, submitted (arXiv:0909.1570)
Ferreira, J. 2007, Lecture Notes in Physics 723 (Berlin: Springer), 181
Field, G. B., & Rogers, R. D. 1993, ApJ, 403, 94
Fleming, T. P., Stone, J. M., & Hawley, J. F. 2000, ApJ, 530, 464
Frank, J., King, A., & Raine, D. J. 2002, Accretion Power in Astrophysics (3rd ed.; Cambridge: Cambridge Univ. Press)
Fromang, S., & Papaloizou, J. 2007, A&A, 476, 1113
Fromang, S., Papaloizou, J., Lesur, G., & Heinemann, T. 2007, A&A, 476, 1123
Haardt, F., & Maraschi, L. 1993, ApJ, 413, 507
Hawley, J. F., Gammie, C. F., & Balbus, S. A. 1995, ApJ, 440, 742
Hawley, J. F., Gammie, C. F., & Balbus, S. A. 1996, ApJ, 464, 690
Hirose, S., Krolik, J. H., & Blaes, O. 2009, ApJ, 691, 16
Kuncic, Z., & Bicknell, G. V. 2004, ApJ, 616, 669
Landau, L. D., & Lifshitz, E. M. 1987, Fluid Mechanics (Oxford: Pergamon Press)
Lesur, G., & Longaretti, P. Y. 2007, MNRAS, 378, 1471
Lynden-Bell, D. 1969, Nature, 223, 690
Merloni, A., & Fabian, A. C. 2002, MNRAS, 332, 165
Miller, K. A., & Stone, J. M. 2000, ApJ, 534, 398
Moreno-Insertis, F. 1986, A&A, 166, 291
Mushotzky, R. F., Done, C., & Pounds, K. A. 1993, ARA&A, 31, 717
Nowak, M. A. 1995, PASP, 107, 1207
Pariev, V. I., Blackman, E. G., & Boldyrev, S. A. 2003, A&A, 407, 403
Pessah, M. E., Chan, C. K., & Psaltis, D. 2006, MNRAS, 372, 183
Pessah, M. E., Chan, C. K., & Psaltis, D. 2007, ApJ, 668, L51
Pessah, M. E., & Goodman, J. 2009, ApJ, 698, L72
Sano, T., & Inutsuka, S. I. 2001, ApJ, 561, L179
Sano, T., Inutsuka, S. I., Turner, N. J., & Stone, J. M. 2004, ApJ, 605, 321
Schramkowski, G. P., & Torkelsson, U. 1996, A&AR, 7, 55
Shakura, N. I., & Sunyaev, R. A. 1973, A&A, 24, 337
Shi, J.-M., Krolik, J. H., & Hirose, S. 2009, ApJ, submitted (arXiv:0909.2003)
Stone, J. M., Hawley, J. F., Gammie, C. F., & Balbus, S. A. 1996, ApJ, 463, 656
Suzuki, T. K., & Inutsuka, S.-I. 2009, ApJ, 691, L49
Velikhov, E. P. 1959, JETP, 36, 1398
Vishniac, E. T. 1995, ApJ, 451, 816
Vishniac, E. 2009, ApJ, 696, 1021
Wang, J.-M., Watarai, K.-Y., & Mineshige, S. 2004, ApJ, 607, L107
Wang, Y.-M., & Sheeley, N. R., Jr. 2003, ApJ, 599, 1404